ELSEVIER

Powder Technology 124 (2002) 188–194

POWDER TECHNOLOGY

www.elsevier.com/locate/powtec

In-line structure measurement of food products

F.G.C. Bijnen [a,*], H. van Aalst [a], P.-Y. Baillif [a], J.C.G. Blonk [a], D. Kersten [a], F. Kleinherenbrink [a], R. Lenke [b], M.L.M. vander Stappen [a]

[a] *Unilever Research Vlaardingen, P.O. Box 114, 3130 AC Vlaardingen, The Netherlands*
[b] *University of Konstanz, P.O. Box 5560, D-78457 Constance, Germany*

Abstract

Changes in the supply chain design for the food industry resulted in a set of requirements for the process sensors of the structured products. Some examples of sensors, which could fulfill these requirements, are discussed. © 2002 Published by Elsevier Science B.V.

Keywords: In-line; Process measurement; Ultrasound; Backscattering; State of phase; Particle size; Foods

1. Introduction

Important trends in the consumer behaviour for the upcoming 10 years which will change the supply chain design are: (i) an increased need for individual solutions, (ii) improved health and (iii) immediate product availability. These drive an ever more rapidly changing portfolio of products and product structures of improved quality. Low levels of stock, rapid changeover capabilities, fast market introduction and late customisation are required. The drive for the enhanced flexibility while delivering an ever-increasing level of quality and service sets the scene for future process measurement needs.

The current assembly of equipment in food factories has largely been developed based on tradition and driven by the need to deliver a constant product quality. Structural and textural properties are generally determined off-line on finished products. Although the need for this type of dedicated manufacturing will not fade away and will concentrate on high volume and few changeovers, there is a growing need for the increased flexibility and for the introduction of the novel designed microstructures which need more mild and new processing regimes. The development of these new processing regimes requires more understanding of the structure–process–equipment relationships.

Raising the level of understanding for the process development and raising the flexibility in the factory involves advanced process measurement capabilities. In this paper, the requirements and some options to fulfil these required measurement capabilities will be presented along a framework on how to characterise microstructures.

2. Requirements on process sensors for structured products

One can distinguish two types of process sensors feeding the above mentioned requirements.

(i) Laboratory and pilot plant sensors are built to understand the microstructure formation processes. Tools for measuring and describing the microstructure during the formation are therefore the key. These sensors should allow to validate the models describing the microstructure evolution. The measured structure parameters should preferably have absolute accuracy.

(ii) Sensors which allow the improved control of a flexible manufacturing process with a fast-changing product portfolio. To allow for the rapid Quality Assurance (QA), these sensors should be able to give absolute values of the product quality parameters without too much calibration and cross-correlation. When flexibility is led to the extremes, one cannot adopt the traditional chemical engineering approach to monitor the changes in the process in-line and link these to the off-line (analytical) signals anymore.

3. Framework for the description of microstructures

A proper description of the microstructure is required for two main reasons. The microstructure is formed by the

* Corresponding author.
E-mail address: frans.bijnen@unilever.com (F.G.C. Bijnen).

0032-5910/02/$ - see front matter © 2002 Published by Elsevier Science B.V.
PII: S0032-5910(02)00018-9

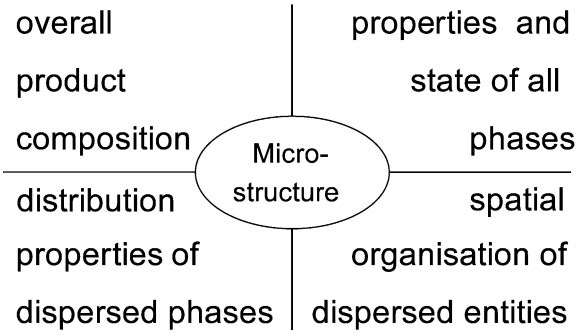

Fig. 1. Framework of the four attributes of a microstructure.

phenomena, which take place in the manufacturing process, and it determines, to a large extent, the perception of the consumer.

A consumer panel will experience food products in subjective terms like the appearance or mouthfeel. These attributes can often be quantified in objective properties like colour or rheology. The relation between these properties and the underlying microstructure is often complex in nature. Note that also for the process control, these relationships are of some importance since the physico-chemical phenomena in the production process need to be targeted to create a microstructure with the desired consumer attributes in the end.

A multiphase microstructure can be described by the specific parameters of each of the phases, interfaces and the spatial organization. The upper part in Fig. 1 gives the type of molecules, their physical state (solid, gas, liquid) and their properties (viscosity, water binding capacity, etc.). The lower part describes the distribution properties of the dispersed phase(s) (shape, size distribution, interface, charge) and their (3D) spatial arrangement.

4. Overall product composition

The four main components of food are water, carbohydrates, fats/oils and proteins. Usually, the chemical composition of a food product hardly changes during the processing; fermentation being a noticeable exception. Nevertheless, the exact composition is almost never known. Natural ingredients can vary due to seasonal and economic purchase reasons. The effects of the varying ingredients on the final product microstructure and on the in-line measurement result can therefore be troublesome.

In-line monitoring of the composition of products could become important in a flexible process environment to allow a rapid changeover, minimum waste and guaranteed quality. Most successful techniques in this area for the in-line process measurement operate in the radiofrequency/microwave and NIR region. The use of neural nets and other black box techniques for the interpretation has increased the accuracy drastically, however, the need for the laborious calibration procedures may hamper their introduction for the QA in flexible manufacturing.

5. Properties and state of all phases

The physical phases of the components of a food product are strongly determined by the temperature or temperature history of the product resulting in a solid, liquid or gas phase. Cooling induces the crystallisation of water and fat and the gelation of biopolymers. Heating induces the denaturation and coagulation of proteins. Phase changes take time and are often not complete when the product is filled in the final assembly (e.g. in a tub of margarine). The measurement of the state of phase is therefore mainly of importance to gain more understanding of the physico-chemical phenomena in relation to the composition and for the (traditional) process control.

Example 1: Solid phase by ultrasonic velocity. Oil crystallisation takes place when the liquid oil undergoes a temperature decrease and becomes supersaturated. The level of solids can be determined by the ultrasonic velocity measurements. The basis for the measurement is the large difference in the speed of sound (approximately 2000 m/s) in the fat phase as compared to the liquid phase (approximately 1400 m/s) [1]. The speed of sound as a function of temperature varies substantially for any different fat blend. For an industrially useful accurate determination of solids, the measurement system should be independent of the changes in the composition of the fat blend. For a batch system, the solution resides in monitoring the speed of sound as a function of temperature and direct extrapolation of the information that was found about the temperatures at which crystallisation takes place. To this end, we immersed an ultrasonic pulse echo system (see Fig. 2) inside a batch crystalliser. A pulse of sound at 2 MHz is sent into the slurry by a piezotransducer. In between the transducer and the

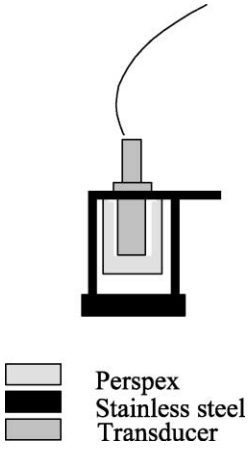

Fig. 2. Ultrasonic pulse echo speed of sound measurement system. The product flows in between the Perspex rod and the stainless steel backplate.

slurry, a piece of Perspex is positioned. After travelling a distance of 10 mm in the slurry, the pulse is reflected back from a stainless steel backplate. The same transducer monitors the reflected pulse. The travelling time gives the speed of sound in the slurry. The choice for the frequency and distance is given by the required accuracy (high frequency, large distance), level of acoustic absorption (low frequency, short distance) and practical measurement circumstances (large distance).

In Fig. 3a, between 13 and 15 h, a change in the temperature from 62 to 26 °C corresponds to a change in the speed of sound of the liquid fat from 1330 to 1440 m/s. The slope of -3 m/s K is typical for the liquid fats. After 15 h, the oil starts to crystallise during the further slow decrease of the temperature. The increase in the speed of sound is mainly due to the fat crystal formation. The level of fat crystals can be determined from the measured speed of sound after the extrapolation of the speed of sound of the liquid and an estimation of the speed of sound of the solid (taken at 2000 m/s) [2]

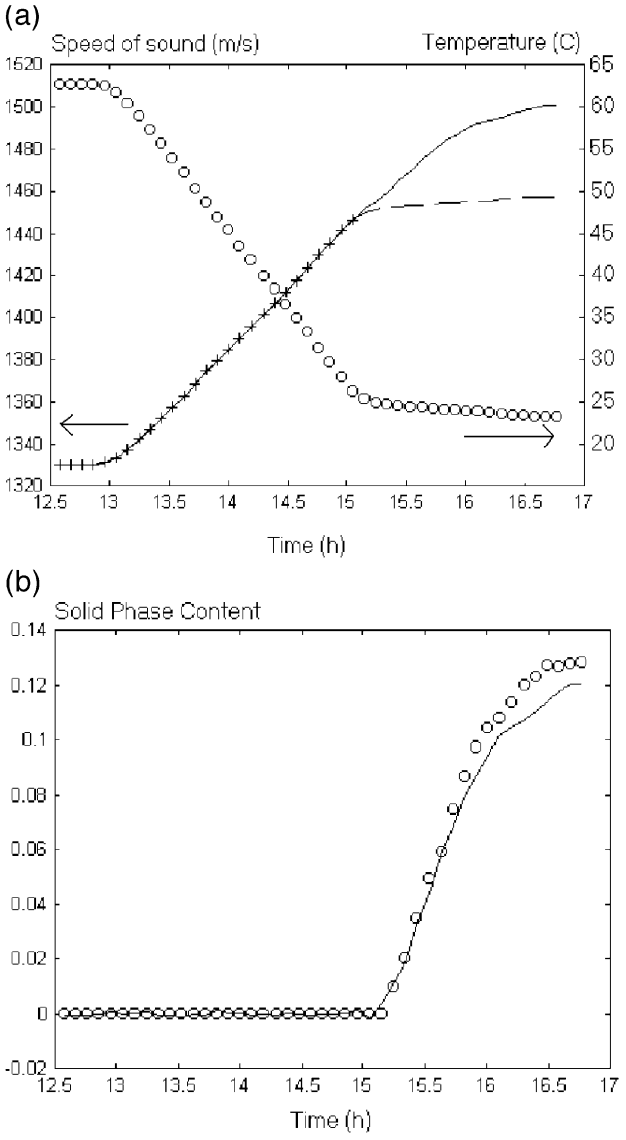

Fig. 3. (a) Ultrasonic monitoring of velocity changes during a batch experiment in crystallising oil at 2 MHz (solid line). After 15 h, the oil starts to crystallise and become a slurry. The dotted line represents the extrapolated velocity of the pure liquid oil. The open circles represent the temperature. (b) From the difference between the speed of sound of the slurry and the speed of sound of the oil in (a) the solid fat contents can be determined (solid line). The circles represent off-line NMR measurements for the validation of the solid fat content determination by ultrasound.

$$\phi = \frac{\frac{1}{C^2} + \frac{1}{C_l^2}}{\frac{1}{C_s^2} + \frac{1}{C_l^2}} \tag{1}$$

with ϕ = solid phase content, C = measured speed of sound, C_s = speed of sound of the solid, C_l = speed of sound of the liquid.

The calculated solids levels from Eq. (1) are compared with the rapid off-line pulsed NMR method. As shown in Fig. 3b, a good correspondence is obtained.

For an in-line measurement of the solids in a *continuous* process line with a fast crystallising blend (e.g. margarine), the challenge is to know the speed of sound of the liquid at the temperature of the solid phase contents determination without the need for trials/calibrations when a new fat blend is used.

Example 2: Gelation by ultrasonic absorption. Cooling causes the gelation to take place in a suitable biopolymer solution. We employed an ultrasonic absorption monitor to obtain understanding on the gelation process [3]. Similarly, as with the solid fat monitor, a pulse of the acoustic energy is sent to the product. Acoustic absorption due to gelation increases to higher frequencies. For sensitivity reasons and for subsequent application in a continuous process line (results not shown), a frequency of 60 MHz was chosen.

The setup employed here to monitor the gelation in a batch arrangement was based on transmission. Quartz was employed as the material between the settling gel and the transducers because of its high transparency for the high frequency acoustical waves. The decrease in amplitude of a transmitted acoustical pulse is directly related to the attenuation $\Delta\alpha$ in the gel.

The measured attenuation can be converted into the loss part of the rheological longitudinal modulus M'', according to Ref. [4]

$$M'' = 2\rho v_l^3 \frac{\alpha}{\omega} \tag{2}$$

with v_l = speed of sound for the longitudinal waves, ρ = dendensity of liquid, α = acoustic absorption for the longitudinal waves, ω = the angular wave frequency.

Fig. 4 shows the evolution of the gelation expressed as the loss modulus M'' on a nonmoving settling biopolymer solution monitored at 60 MHz. The empirical link found between the ultrasound and low frequency (0.6 Hz) rheol-

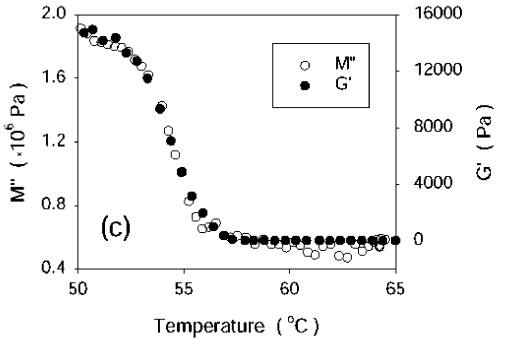

Fig. 4. Ultrasonic monitoring of nonmoving settling gelation of a biopolymer solution by changes in the product attenuation at 60 Mhz (M'') compared to the low frequency (0.6 Hz) rheological data of a similar experiment (G').

ogy (G' : elastic part of the shear modulus), obtained from a separate experiment, cannot yet be explained from the underlying physics. Nonetheless, it is robust against the changes in the concentration and temperature history. For some biopolymers, the level of salt disturbs the robustness of the relation. To allow the technique to become more robust, a better understanding on the empirical relation, which has been found, is required. Shearing, at the same time, cooling, results in a particulate structure known as the shear gel. How the gel properties develop in the production equipment is under scrutiny.

6. Distribution properties of dispersed phases and their spatial arrangement

In addition to the properties of the phases, the dispersed phase(s) can be characterised by the properties of the distribution. The distribution of entities consisting of the local homogeneous zones of the single-phased material (typically 100 nm to 100 μm) can be characterised by the size distribution, shape, interface with the continuous phase, and for example, the electrical charges of the entities.

The resulting microstructure from a phase change is strongly determined by the applied shear. For the oil and water emulsions, the main process determinant of the size distribution is the time–shear profile.

The field of characterisation of the spatial arrangement of particles and interconnecting networks is not well-developed. It suffers from the lack of mathematical characterisation tools and (in-line) measurement techniques. However, the fact that the process measurement devices can monitor systems could offer additional advantages with respect to the analytical systems. For example, it may become possible to describe the deformation of the microstructure under the shear resulting from the flow.

Example 3: Mean droplet sizes by coherent and diffusive backscatter. The diffusive path length l^* of (multiple scattered) photons in highly concentrated emulsions (up to 80% oil in water) can be related back to the mean droplet/particle size [5,6]. The advantage of the *coherent* backscatter is that it can monitor remotely and is therefore extremely flexible.

In a somewhat simplified view, coherent backscattering can be understood as follows. When a coherent laser beam enters a turbid material, the photons start diffusive pathways through the medium and are scattered out of the product in all directions (diffusive scattering). Some of these pathways result in scattering exactly back into the incident laser beam. These pathways can be travelled in both opposite directions yielding (almost) a doubling of the scattered intensity in the direction counter to the incident beam. The angular width of this coherently scattered beam depends on the amount of scattering in the medium. A shorter l^* results in the shorter distances between the entrance/exit points of the double-entry pathways and therefore results in a larger angular width. The angular width of the coherent backscatter beam is monitored by a CCD camera and can be converted into a value for l^*. The experimental setup is given in Fig. 5.

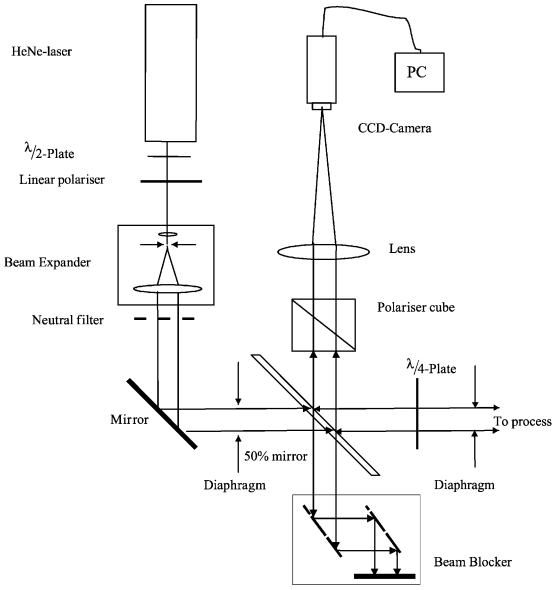

Fig. 5. Coherent backscatter setup. As an illuminating source, we used a He–Ne laser with an output power of 35 mW and a wavelength of 633 nm. The intensity of the laser is controlled by a λ/2-plate and a linear polariser. In order to illuminate a big area of the sample, we expanded the laser beam diameter up to 1.2 cm with a beam expander. Afterwards, the laser beam passes through a diaphragm to define the illuminated region and a semitransparent mirror under 45°, where half of the light is reflected. This part of the light must be completely absorbed, reflection included. This is performed by the neutral filter. In order to neglect single scattering, all measurements are performed in parallel circular channel, which means that the incident and detected light have the same state of circular polarisation. To do this, a λ/4-plate is placed between the semitransparent mirror and the measurement zone in the process. A second diaphragm determines the backscattered region. The backscattered light reflected at the semitransparent mirror is then detected by a polariser cube, which is aligned parallel to the linear polariser plate.

An empirical relation for l^* with droplet size in highly concentrated emulsions was obtained by impinging the laser beam of a coherent backscatter setup onto the wall of a cylindrical glass vessel containing 50% oil, 50% water and 0.1% emulsifier. A high shear-mixing device was employed for the emulsification. At specific times, the measurements on the coherent backscatter cone were recorded. At the same time, some emulsion was removed for the off-line evaluation (dilution, electrozone) of the droplet size distribution. By taking into account the refractive index difference between the oil and water phase multiple scattering, the Mie theory can be employed to calculate l^* as a function of the "average" droplet size. The results are given in Fig. 6. Well above sizes of the optical wavelength larger l^* correspond to larger droplet sizes (as for the diluted case: Fraunhofer scattering). The theoretical results show, however, that around 1 μm, the relation is not monotone anymore (Mie scattering zone). Far below 1 μm (Raleigh), smaller droplets will give rise to larger l^*. The robustness and further quantification of this relation in the 1–20 μm zone is subject to further scrutiny. Developments in the multiple scattering Mie-theory will also allow the linking droplet sizes above 5 μm directly with the diffusive path length. The recent commercial availability of a non-remote *diffusive* backscatter instrument (Turbiscan, Formulaction) also allows to determine the diffusive photon path length l^* in relation to the in-line droplet size. This instrument could speed up the quantification of this relation and aid the process understanding at the laboratory/pilot plant scale [7]. Note, however that for both systems, it is necessary to compensate for the changes in the refractive index of the two materials forming the emulsion.

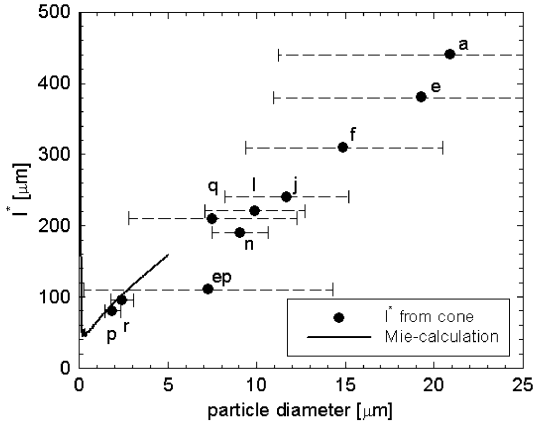

Fig. 6. Diffusive photon path length l^* as determined by the coherent backscatter in a 50% oil in water emulsion as the function of the average droplet size ($D_{3,2}$) determined by the electrozone method (Coulter). The horizontal bars reflect the width of the size distribution. Although the correlation is quite satisfactory, the l^* of bimodal sample ep (50% of sample e and 50% of sample p) indicates that the ($D_{3,2}$) may not be the best parameter to link l^* to. Mie-calculations show good correlation up to 5 μm.

Example 4: Mean droplet sizes by the Focused Beam Reflectance Measurement (FBRM). The Lasentec Company has mainly developed its FBRM to monitor the relative changes in the structural parameters and has shown to be very successful in that. For relatively large particle sizes (sup 50 μm), an analytical link between the cord length and particle size has been found [8]. In view of the requirements put forward above, we made a study on the use of the Lasentec FBRM and its window of applicability on monitoring the absolute droplet sizes in the 1–20 μm size ranges.

The Lasentec FBRM employs a diode laser of which the focus is scanned through a medium containing particles. In the highly scattering media, the ideal position of the focus is located in the sapphire window close (within 10 μm) to the interface with the product. When the focus crosses a particle, a reflection is detected. The reflection gives a so-called cord length. Since the point of crossing on a specific particle can vary, a single particle size will result into a specific cord length distribution. For the ideal case of a single spherical particle, the resulting cord length distribution can easily be calculated. Therefore, in a simple first approximation from the measured cord length distribution in a real system, the droplet size distribution can be deduced [6].

We correlated the various cord length representations with the droplet size representations as determined by the electrozone after dilution. We checked the robustness of the measurement by varying the refractive index of the oil phase, the concentration of the oil, size (1–20 μm) and size distribution of the droplets and the effect of clustering. For this, the Lasentec FBRM was immersed in a vessel containing a shearing device. Unfortunately, an analytical link in this size range between the cord length distribution and the droplet size distribution could not be found. However, we were able to establish an empirical link with a restricted window of applicability. From Fig. 7a and b, it becomes clear that for establishing an empirical link between the Coulter electrozone and Lasentec FBRM, it is crucial to determine the proper distribution moment for comparison [9]. We found that the mean unweigthed cord length of the FBRM was fairly independent of the size distribution and type of food oil used when linked to the $D_{3,2}$. There was a weak dependence on the concentration and a strong dependence on the rate of clustering.

For a 50% oil in water emulsion, excluding the effect of clustering and the contribution of sizes below 5 μm, a mean unweigthed FBRM cord length of 6.8 μm resulted in a $D_{3,2}$ value of 10 ± 3.3 μm ($n = 13$, 95% confidence limit). For concentrations higher than 50% o/w, we also found that the speed at which the product was flowing in front of the window of the Lasentec affected the cord length distribution. This may be due to deformation of the droplets in the shear field.

Example 5: Shape and size by 2D and 3D in-line imaging. Techniques that allow the determination of the

particle size distribution, their shape and the arrangement of particles require a 2D or 3D imaging technique. For this, we have employed an off-line method, which was put "semi" in-line. A miniature process vessel was put on top of the window of a Confocal Laser Scanning Microscope (CSLM) to study the structure evolution of a dairy texture. The measurement could only be performed when the product was not flowing so the process had to be stopped for a few seconds for the measurement to take place. The method gives the sizes and particle shape information expressed in fractal numbers (see Fig. 8).

Further development of the CSLM technique to larger scale processes is not in the line of expectation. For proper CSLM measurements, dyes are required and the confocal character hardly allows a flowing product. However, 2D imaging techniques in combination with the rapid analysis could offer a more robust information on the particulate size distribution, their arrangement and even the evolution of structure under shear. Commercial in-line imaging sensors have a limited applicability towards characterising a wide range of microstructures. One can monitor bubbles with such an instrument (e.g. Lasentec PVM) but it is not yet possible to quantify sizes in highly concentrated emulsions

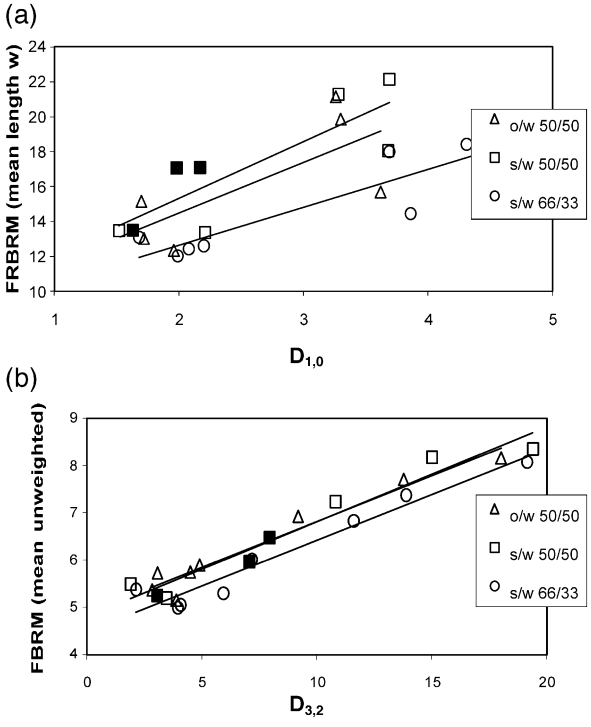

Fig 7. (a) $D_{1,0}$ versus the mean length weighted cord and (b) $D_{3,2}$ versus the mean unweighted cord. Different Lasentec FBRM cord length representations versus the different mean droplet size distribution parameters ($D_{1,0}$ and $D_{3,2}$) as determined by the electrozone method. The choice for the proper representation of the distribution strongly affects the success of a correlation. Sunflower oil in water is s/w and o/w is for olive oil in water. Dimensions are in μm.

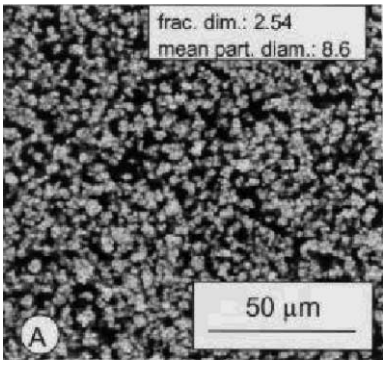

Fig 8. CSLM micrograph of a dairy texture microstructure. Particle size, shape, and configuration can be determined simultaneously.

containing droplets in the sub 20-μm range. Rapid and robust image analysis is another field of scrutiny before reliable application of these types of instruments can be performed.

7. Outlook

Considering the changes in the behaviour of consumers, some effects for the design of the supply chain and manufacturing operations have been given followed by their implications for the process sensors of the structured products in the Fast Moving Consumer Goods (FMCG) food industry. An overview of some potential candidates for the in-line structure measurement and their limitations has been shown.

- Sensors to monitor the composition (moisture, fat content, etc.) currently achieved a relative accuracy of 0.1–1%. These are often sufficient but the calibration procedures (if any) in a rapid changing product portfolio should be minimal.
- Sensors to monitor the state of phase will mainly be used to build increased process understanding for the development of the novel processes and for process control. Options for monitoring the state of phase properties by laser-based acoustic pulse sources and detectors show potential for development because of the increased flexibility due to the remote sensing. However, in-line QA will often be difficult because the final state of phase (rate of crystallisation or gelation) of food products is often formed after the filling operation and during storage.
- Although the options for the absolute quantification are present, current in-line particle size options have demonstrated only a qualitative relation to the droplet size. Only by calibration (empiricism), an attempt can be undertaken to get a quantitative relation in a restricted window of variables. For a rapid changing product portfolio and variable ingredients, these qualifications may prove insufficient. Both the process understanding and particle size distribution control in a flexible factory environment require quantitative information. In-line imaging and image analysis could fulfil

this requirement. Closely monitoring this information to the final product assembly would allow process control and QA at the same time.

- The area of the particle arrangement inside a product matrix is still too young and unexplored for having major implications on the requirements of the process measurement instrumentation.

References

[1] D.J. McClements, M.J.W. Povey, Comparison of pulsed NMR and ultrasonic velocity techniques for determining solid fat contents, Int. J. Food Sci. Technol. 23 (1988) 159–170.
[2] C.A. Miles, G.A.J. Fursey, C.D. Jones, Ultrasonic estimation of solid/liquid ratios in fats, oils and adipose tissue, J. Sci. Food Agric. 36 (1985) 215–228.
[3] M. Audebrand, J.L. Doublier, D. Durand, J.R. Emery, Investigation of gelation phenomena of some polysaccharides by ultrasonic spectroscopy, Food Hydrocolloids 29 (1995) 195–203.
[4] R.T. Beyer, S.V. Letcher, Physical Ultrasonics, Academic Press, New York, 1969.
[5] R. Lenke, G. Maret, Multiple scattering of light: coherent backscattering and transmission, in: W. Brown, K. Mortensen (Eds.), Scattering in Polymeric and Colloidal Systems, Gordon and Breach, Reading, UK, 2000, pp. 1–72.
[6] A. Dogariu, J. Uozumi, T. Asakura, Particle size effects on optical transport through strongly scattering media, Part. Part. Syst. Charact. 11 (1994) 250–257.
[7] B. Abismail, J.P. Canselier, A.M. Wilhelm, H. Delmas, C. Gourdon, Emulsification by ultrasound: drop size distribution and stability, Ultrasonics 6 (1999) 75–83.
[8] A. Tadayyon, S. Rohani, Determination of particle size distribution by Partec 100: modeling and experimental results, Part. Part. Syst. Charact. 15 (1998) 127–135.
[9] M. Alderliesten, Mean particle diameters. Part I: evaluation of definition systems, Part. Part. Syst. Charact. 7 (1990) 233–241.